2015 American Control Conference
Palmer House Hilton
July 1-3, 2015. Chicago, IL, USA

Robust Tracking/Impedance Control: Application to Prosthetics*

Hadis Mohammadi[1] and Hanz Richter[2]

Abstract— **Stability and human-like motion are among the main factors that should be considered while designing a prosthetic limb. The prosthetic limb should be capable of accommodating environmental forces. The existence of parametric uncertainties has raised the need for robust stability and performance of the prosthesis. In this paper, a mixed tracking/impedance robust controller is developed based on passivity techniques. The controller is developed for general robotic manipulators and then applied to a powered knee/ankle prosthesis model attached to a robotic testing machine. Tracking control is used for the hip and thigh links of the test robot, while impedance control is used for the knee and ankle joints of the prosthesis. The dynamics resulting from the interaction between robot and environment are stabilized by specifying a suitable target impedance. The robust passivity framework was used to derive a joint space controller. A Lyapunov function is used to show that the tracking errors of the motion-controlled joints approach zero, while the impedance of the remaining joints approaches the designed target. A simulation study shows how impedance parameters can be used to trade off reference tracking of the impedance-controlled joints and interaction forces.**

I. Introduction

Impedance control is a technique for the regulation of dynamic interaction between a manipulator and its environment. This technique is used in applications such as object manipulation, industrial robotics and prosthetic applications demanding a smooth motion to avoid impact between the manipulator and the object or the environment. In this method of control, the environment is considered as an admittance (returning forces in response to motion inputs) and the manipulator as an impedance (returning motions in response to applied forces) [1], [2], [3].

In the presence of interactions with unpredictable environments, force control and position control alone are inadequate. Controlling the *relationship* between force and velocity (impedance) offers a better solution. The desired manipulator impedance is chosen by tuning the desired inertia, damping and stiffness characteristics. For systems with many degrees of freedom, learning variable approaches, on-line approaches [4], [5], [6] and optimization methods [7], [8] can be used to aid impedance parameter selection. In this paper, a combination of impedance and tracking control techniques is developed for general robotic manipulators interacting with an environment.

The development of powered prostheses has increased within the last decade [9], [10], [16], [17], and simple impedance controls have been successfully applied. For instance, the devices reported in [16], [17] control actuators to achieve a target impedance of the form

$$b\dot{\theta} + k(\theta - \theta_0) = \tau$$

where θ is the joint angle and τ is the joint torque. Parameters b, k and θ_0 are scheduled during the various phases of walking. Note the inertial characteristic cannot be adjusted, and only a constant position parameter θ_0 is available to specify desired joint motion for $\tau = 0$.

The technique presented in this paper includes an adjustable inertial characteristic and a time-varying reference trajectory to be precisely followed by the joint when unloaded. The approach is based on a robot dynamics model, compensating for inertial coupling among the links. Moreover, the proposed controller is robust against model parameter uncertainties.

Although robot-environment interaction occurs in task space, the controller has been developed in the joint space. This avoids difficulties such as the need to compute nonlinear transformations and invert Jacobians.

The paper is structured as follows: Section II presents the mathematical model and develops the controller for general robotic manipulators. The application of the proposed method for a prosthetic leg attached to a robotic testing machine. model and the related dynamic equation of the motion for the robot are given in Section III. The results of the simulation and their analysis are provided in Section IV. Finally, Section V is dedicated to the conclusion.

II. Controller Development

The controller is designed to achieve reference tracking for all joints when interaction forces are zero. When forces arise due to interaction, a subset of joints termed *motion-controlled* (MC) should maintain accurate tracking, while the tracking errors of the remaining joints, termed *impedance-controlled* (IC) respond to environmental forces in a prescribed way, the *target impedance*. The equation of the motion for an n-degree-of-freedom robotic manipulator is given by:

$$M(q)\ddot{q} + C(q,\dot{q})\dot{q} + g(q) + R(\dot{q}) + T_e = u \qquad (1)$$

where $q \in \mathbb{R}^n$ is the vector of joint coordinates, $M(q)$ is the inertia matrix, $C(q,\dot{q})$ is the Coriolis matrix, $g(q)$ is the gravity vector and $R(\dot{q})$ is a generic friction term. The vector of joint control torques is u, and $T_e(q)$ is a term capturing the external forces and torques applied to the manipulator. If $F_e = [F_x, F_y, F_z, M_x, M_y, M_z]^T$ represents the external forces and moments applied at a certain point of the manipulator in Cartesian space and J is the kinematic

*The authors are with Cleveland State University, Mechanical Engineering Department
[1]Doctoral student, hdsmohammadi@gmail.com
[2]Associate Professor, h.richter@csuohio.edu

Jacobian at the same point, $T_e = J^T F_e$. Assuming that the first $n-m$ joints are to be motion-controlled, while the remaining m joints are to be impedance-controlled, partition the joint coordinates as $q^T = [q_{MC}^T \quad q_{IC}^T]$. Also partition T_e along MC and IC coordinates as $T_e^T = [T_M^T \quad T_I^T]$. Let $q^d(t)$ represent a set of reference trajectories for the joints and define the tracking error as $\tilde{q} = q - q^d$. The following target impedance is considered in this paper:

$$I\ddot{\tilde{q}}_{IC} + b\dot{\tilde{q}}_{IC} + k\tilde{q}_{IC} = -T_I \tag{2}$$

where I, b and k are diagonal matrices of impedance parameters. Note that $-T_I$ represents the effect of the external forces and moments on the impedance-controlled joints.

Clearly, asymptotic tracking will be achieved also for the IC joints if $F_e = 0$. Otherwise, I, b and k may be tuned to govern the response of $\tilde{q}_{IC}$ to external forces. These control objectives may be achieved by an inverse dynamics approach. However, this method is not applicable in practice due to uncertainties in the model parameter. This motivated the use of the passivity-based approach described in [11], [12], which exploits two structural properties of Eq. 1. The skew-symmetry property establishes that $\dot{M} - 2C$ is a skew-symmetric matrix. This property is used to prove that the system satisfies the passivity property. The linearity-in-parameters property implies that Eq. 1 can always be written as

$$Y(q, \dot{q}, \ddot{q})\Theta = u - T_e$$

where Y is the regressor and Θ is a parameter vector. The regressor is independent of model parameters. The minimum number of parameters required for a linear representation may be found for a given robot configuration. Assume that only an estimate Θ_0 is available, such that the parameter error $\tilde{\Theta} = \Theta - \Theta_0$ is bounded as $||\tilde{\Theta}|| \leq \rho$, for some known $\rho > 0$.

A dynamic compensator with state z is introduced to achieve impedance control. This follows the approach used in previous work on variable-structure methods for robust impedance control, for instance [13]. Let the dynamic compensator have the form:

$$\dot{z} = Az + K_p\tilde{q}_{IC} + K_d\dot{\tilde{q}}_{IC} + K_f T_I \tag{3}$$

where A a Hurwitz and K_p, K_d and K_f will be determined below. In the spirit of robust passivity-based control (RPBC) [11] of manipulators, consider a control input of the form:

$$\begin{aligned} u &= \hat{M}(q)a + \hat{C}(q, \dot{q})v + \hat{g} - Kr + T_I \\ &= Y(q, \dot{q}, v, a)\hat{\Theta} - Kr + T_I \end{aligned} \tag{4}$$

where $\hat{\Theta}$ is an adjustable quantity yet to be determined and vectors a, v and r are partitioned as $a^T = [a_{MC}^T \quad a_{IC}^T]$, $v^T = [v_{MC}^T \quad v_{IC}^T]$ and $r^T = [r_{MC}^T \quad r_{IC}^T]$. Here, a_{MC}, v_{MC} and r_{MC} are defined as in the standard RPB motion control approach and a_{IC}, v_{IC} and r_{IC} include an additional term designed to achieve the impedance control objective.

$$\begin{aligned} v_{MC} &= \dot{q}_{MC}^d - \Lambda_M \tilde{q}_{MC} && (5)\\ a_{MC} &= \dot{v} = \ddot{q}_{MC}^d - \Lambda_M \dot{\tilde{q}}_{MC} && (6)\\ r_{MC} &= \dot{q} - v = \dot{\tilde{q}}_{MC} + \Lambda_M \tilde{q}_{MC} && (7)\\ v_{IC} &= \dot{q}_{IC}^d - \Lambda_I \tilde{q}_{IC} - F_r z && (8)\\ a_{IC} &= \dot{v} = \ddot{q}_{IC}^d - \Lambda_I \dot{\tilde{q}}_{IC} - F_r \dot{z} && (9)\\ r_{IC} &= \dot{q} - v = \dot{\tilde{q}}_{IC} + \Lambda_I \tilde{q}_{IC} + F_r z && (10) \end{aligned}$$

where Λ_M, Λ_I and F_r are diagonal matrices of positive gains. Note that T_e is assumed to be known accurately. This is justified, since external forces may be measured with sensors and the kinematic Jacobian is a function of joint positions and length parameters, which can be measured with high accuracy. Note that $a = \ddot{q} - \dot{r}$ and $v = \dot{q} - r$. Substituting control law 5 into the plant model and dropping the dependence on q from the notation gives:

$$\begin{aligned} M\dot{r} + Cr + Kr &= (\hat{M} - M)a + (\hat{C} - C)v + \\ &\quad (\hat{g} - g) + (\hat{R} - R) \\ &= Y(q, \dot{q}, v, a)(\hat{\Theta} - \Theta) \end{aligned} \tag{11}$$

As shown below with a Lyapunov function, r and $\dot{r}$ converge to zero. If $r = 0$ and $\dot{r} = 0$ are imposed on Eq. 10 and its derivative, the following is obtained:

$$\begin{aligned} z &= -F_r^{-1}(\dot{\tilde{q}}_{IC} + \Lambda \tilde{q}_{IC}) \\ \dot{z} &= -F_r^{-1}(\ddot{\tilde{q}}_{IC} + \Lambda \dot{\tilde{q}}_{IC}) \end{aligned}$$

Using the definition of $\dot{z}$ from Eq. 3 gives:

$$\begin{aligned} F_r^{-1}\ddot{\tilde{q}}_{IC} + (F_r^{-1}\Lambda_I - AF_r^{-1} + K_d)\dot{\tilde{q}}_{IC} &+ \\ (A\Lambda_I + K_p)\tilde{q}_{IC} &= -K_f T_I \end{aligned} \tag{12}$$

which matches the form of the target impedance. Clearly, K_p, K_d, K_f and F_r can always be tuned to yield the desired impedance. Indeed, given desired inertia I, damping b and stiffness k parameters, the gains can be calculated as below:

$$\begin{aligned} F_r &= I^{-1} \\ K_p &= k + AI\Lambda_I \\ K_d &= b - I\Lambda_I + AI \end{aligned}$$

Substituting $r = 0$ in Eq. 7 shows that the motion controlled joints achieve asymptotic reference tracking. Therefore, it only remains to show that r converges to zero with control law 5, provided $\hat{\Theta}$ is suitably chosen. As in standard RPBC, adjust $\hat{\Theta}$ according to:

$$\widehat{\theta} = \theta_0 + \delta\theta \tag{13}$$

where $\delta\theta$ is an additional control term selected with Lyapunov methods. Indeed, consider the Lyapunov function candidate

$$V = \frac{1}{2} r^T M(q) r + \tilde{q}_{MC}^T \Lambda K \tilde{q}_{MC}$$

where Λ =diag(Λ_M, Λ_I). The time derivative of V is

$$\dot{V} = r^T M(q)\dot{r} + \frac{1}{2} r^T \dot{M}(q) r + 2\tilde{q}_{MC}^T \Lambda K \dot{\tilde{q}}_{MC}$$

replacing for $M\dot{r}$ from Eq. 11 results in:

$$\dot{V} = -r^T Kr + r^T Y(\tilde{\theta}+\delta\theta) + 2\tilde{q}_{MC}^T \Lambda K \dot{\tilde{q}}_{MC} + \frac{1}{2} r^T (\dot{M} - 2C) r$$

Using the skew symmetry property:

$$\dot{V} = -r_{MC}^T K r_{MC} + 2\tilde{q}_{MC}^T \Lambda K \dot{\tilde{q}}_{MC} - r_{IC}^T K r_{IC} + r^T Y(\tilde{\theta}+\delta\theta)$$

Substituting for r leads to

$$\dot{V} = -e_{MC}^T Q e_{MC} - r_{IC}^T K r_{IC} + r^T Y(\tilde{\theta} + \delta\theta)$$

where $e_{MC}^T = [\tilde{q}_{MC}^T \;\; \dot{\tilde{q}}_{MC}^T]$. The first and second terms are negative-definite. The third term is made negative-definite in the same fashion as standard RPBC. Considering that $||\tilde{\Theta}|| \leq \rho$, $\dot{V} < 0$ is ensured by the following switching law for $\delta\Theta$:

$$\delta\theta = \begin{cases} -\rho \frac{Y^T r}{||Y^T r||} & , \; ||Y^T r|| \neq 0 \\ 0 & , \; ||Y^T r|| = 0 \end{cases}$$

Since V is quadratic and positive-definite in r and $\dot{V}$ is negative-definite, it is concluded that r must converge to zero asymptotically. Even though this leads to true asymptotic stability, it involves chattering. To alleviate chattering, a deadzone implementation may be chosen:

$$\delta\theta = \begin{cases} -\rho \frac{Y^T r}{||Y^T r||} & ||Y^T r|| > \epsilon \\ -\frac{\rho}{\epsilon} Y^T r & ||Y^T r|| \leq \epsilon \end{cases}$$

where $\epsilon > 0$ is a small deadzone parameter. By doing this, asymptotic stability is lost and replaced by the more relaxed property called *uniform ultimate boundedness*. With this property, e_{MC} and r_{IC} are guaranteed to remain in a neighborhood of zero which can be made as small as desired by reducing ϵ. This represents a practical tradeoff between tracking accuracy and impedance regulation against control chattering.

III. Application Example

A robot designed to test above-knee prostheses and a prosthesis prototype are used to illustrate application of the proposed technique. The robot was designed and built at Cleveland State University in collaboration with the Cleveland Clinic [14], [15]. The robot facilitates testing of new prosthetic leg designs without the intervention of human subjects. The robot has two degrees of freedom, namely a hip vertical displacement and a thigh rotation. In one possible test modality, these degrees of freedom are required to track reference trajectories obtained from human motion data. A passive prosthesis attached to the robot is driven by these motions, and its performance observed as it walks on a treadmill. In this paper, we consider the use of a powered ankle-knee prosthesis, however. In this case, the overall system has four degrees of freedom. With the proposed technique, hip and thigh joints are controlled for tracking, while the knee and ankle joints are impedance-controlled.

A. Model

A schematic of the robot is shown in Fig 1, and Fig 2 shows coordinate frame assignments are according to the Denavit-Hartenberg convention. For details about model matrices and parameters, refer to [14]. The prosthesis was modeled as four additional robotic links. A foot model and a ground contact model were also included. As Fig. 3 shows, a triangle geometry is assumed for the foot, with contact points at the toe and heel. At each contact point there is a normal and horizontal ground reaction force. During ground contact, the effect of these forces is reflected on the joints by vector T_e. A treadmill with a compliant belt is used as a walking surface. The stiffness of the belt is used in the vertical force calculation. It is assumed that the robot walks along the $x-$axis. The position and orientation of the foot relative to the belt is known at each moment from forward kinematics and joint coordinate measurements. Contact of either end of the foot (heel or toe) with the belt creates a deflection d_z calculated as:

$$d_z = Z_{\text{standoff}} - Z_{\text{motion}}$$

where Z_{standoff} is the total distance between the base of the foot the origin of the world frame when the leg is standing vertically and fully extended. Z_{motion} is the total distance between the foot end and the origin of the world frame when the leg is in motion. Knowing the deflection and stiffness K_{belt} of the belt, the normal force at the heel or toe can be calculated:

$$F_z = -K_{\text{belt}} d_z \tag{14}$$

To calculate the horizontal friction forces, a coefficient μ between the belt and the foot is considered, so that

$$F_x = \mu F_z \tag{15}$$

These forces are used to assemble F_e for Eq. 1. The vector of joint coordinates is then

$$q = [q_1 \; q_2 \; q_3 \; q_4]^T \tag{16}$$

where q_1 is the transitional displacement of the hip along the z_0-axis, q_2 represents the rotation of the thigh about the z_1-axis, q_3 is the rotation of the knee about the z_2-axis and finally q_4 is the rotation of the ankle about the z_4-axis.

Considering friction in the joints, the parameter vector has twelve components, thus the dimension of regressor matrix is 4×12 which 4 is the total number of dynamic equations for all links or joints (one equation per joint). The parameter vector consists of 12 independent inertia terms which construct a 12×1 parameter vector shown in details in [15]. The objective is to track the motion references for the hip and the thigh using robust tracking control, while using robust impedance control for the knee and the ankle. The reference trajectories are obtained from a subject with a height of 1.829 m and a mass of 78 kg. The reference trajectories correspond to normal walking at a speed of 4.5 km/h.

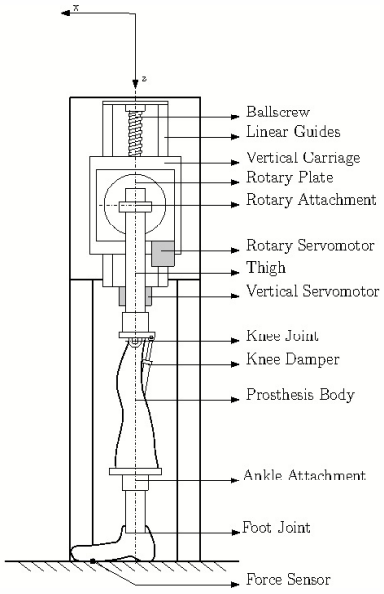

Fig. 1. Schematic of the prosthetic leg

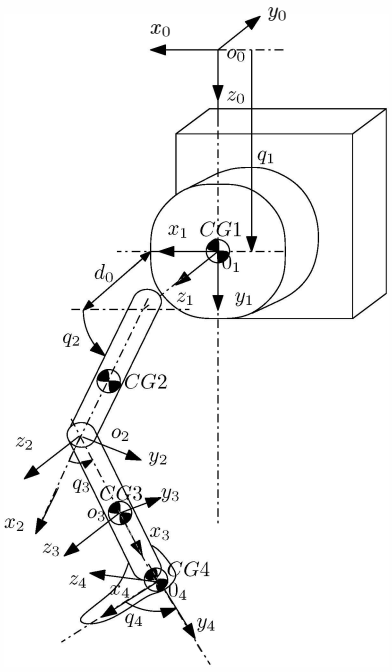

Fig. 2. Frame assignments

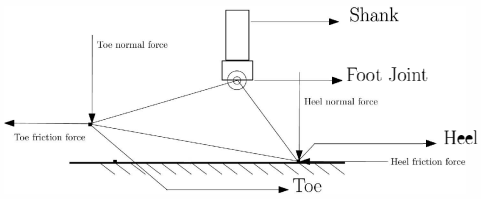

Fig. 3. Schematic of the prosthetic foot model

K	255	155	230	300
Λ	255	150	350	550

TABLE I

CONTROL GAINS USED IN THE SIMULATION STUDY

B. Simulation Results

The mixed robust motion/impedance controller was simulated with a dynamic model of the test robot. The hip and the thigh were required to track the motion references precisely, while some deviation from the reference trajectories for the knee and the foot was allowed in order to avoid producing large contact forces. A mass-spring-damper impedance characteristic was specified for the knee and the ankle. Two sets of results are presented. In both cases, parametric uncertainty was introduced by randomly perturbing Θ so that $||\tilde{\Theta}||$ was 10% of $||\Theta||$. In the first simulation, a relaxed impedance with relatively low damping and stiffness is applied. For the second set, an impedance with higher damping and stiffness is considered. As confirmed by the results, impedance control is a trade-off between trajectory tracking accuracy and the magnitude of the interaction forces. The control gains are the same for both cases and are shown in Table I.

C. Low Impedance Characteristics

The parameters for the low target impedance are shown in Table II. Figures 4 and 6 show the results for low target impedance. As it can be seen from the graphs the first three joints show near perfect tracking while the foot joint displays larger tracking errors due to the influence of the contact forces on the foot. However, this performance is completely acceptable and according to the expectations, since impedance control allows deviations from tracking in order to avoid high contact forces. The square of the tracking error for each joint is also calculated and shown in Fig. 5. The square error will decrease and oscillate between zero and some small peak value after some time. The peak square error over the 5-second simulation is used as an indication of performance. Even though a non-aggressive impedance is utilized, the simulation results show the tracking error at the knee is small, with a peak square error near 2×10^{-3}. The peak square error for the ankle is near 0.1. Also the simulation results show near perfect tracking for the first two joints, with square errors near 8×10^{-7} and 3×10^{-5} since these joints are motion-controlled. The peak vertical forces at the heel and toe are 700 and 900 N.

impedance	knee	foot
I	0.1	0.1
b	150	30
k	1000	400

TABLE II

PARAMETERS FOR LOW IMPEDANCE CHARACTERISTICS

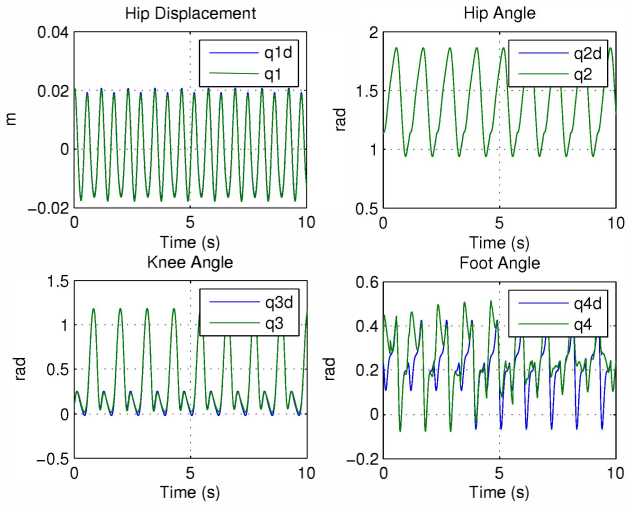

Fig. 4. Joint reference (desired) and actual angles (low impedance)

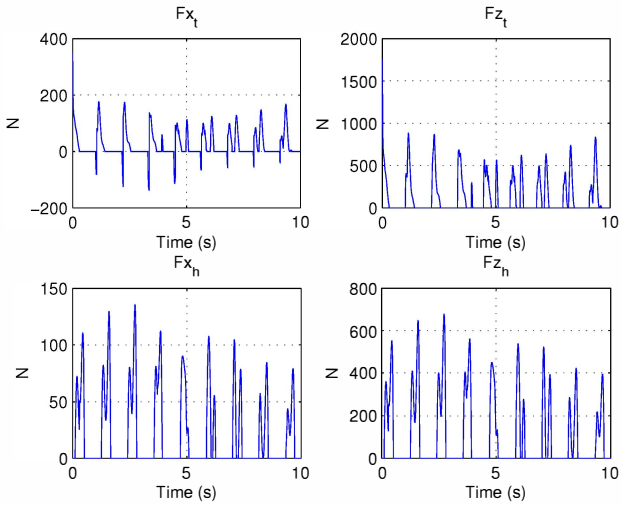

Fig. 6. Ground contact forces in heel and toe (low impedance)

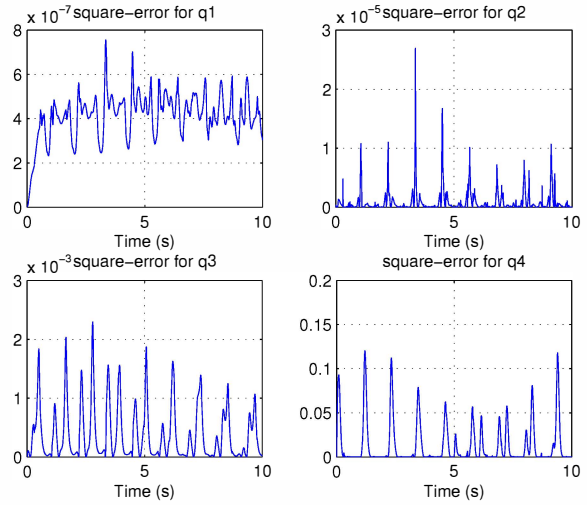

Fig. 5. Square of the tracking error (low impedance)

impedance	knee	foot
I	0.9	0.9
b	500	250
k	3000	2000

TABLE III

PARAMETERS FOR HIGH IMPEDANCE CHARACTERISTICS

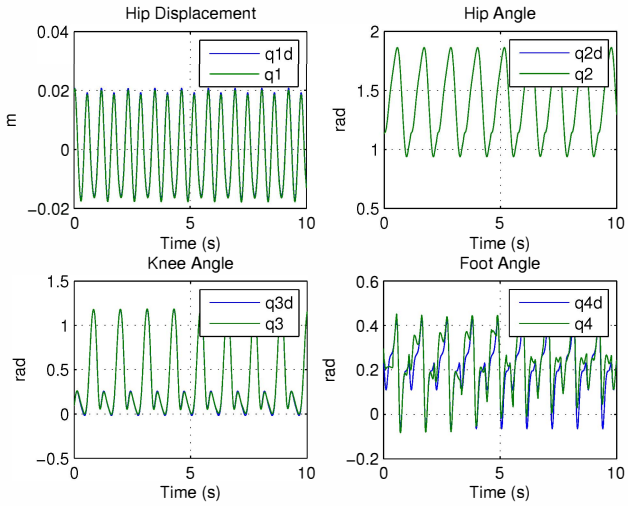

Fig. 7. Joint reference(desired) and actual angles (high impedance)

D. High Impedance Characteristics

The parameters for the high target impedance are shown in Table III. Figures 7 and 9 show the trajectories and the generated forces, and Fig. 8 shows the square tracking errors. In this case, the first two joints have square errors near 8×10^{-7} and 2×10^{-5}, respectively. The tracking at the knee, again, shows a small tracking error, with peak square magnitude near 7×10^{-4}. The ankle however, has a significantly smaller tracking error in comparison with the high impedance case, with a square magnitude near 0.02. As expected, the peak vertical forces at the heel and toe are larger, at 750 and 2000 N.

IV. CONCLUSIONS

In this paper, a mixed tracking/impedance robust controller was developed using the passivity framework. It can be used for industrial robotic manipulators, prostheses and other systems. The tradeoff between tracking accuracy and impact force magnitudes can be conveniently managed by adjusting target impedance parameters. The process of deriving the controller along with its stability proof were presented. The approach allows the use of impedance control or tracking control for all joints as particular cases. The chattering solution ensures that the tracking error of the motion-controlled joints converges to zero, as the impedance-controlled joints attain the target impedance. With the deadzone implemen-

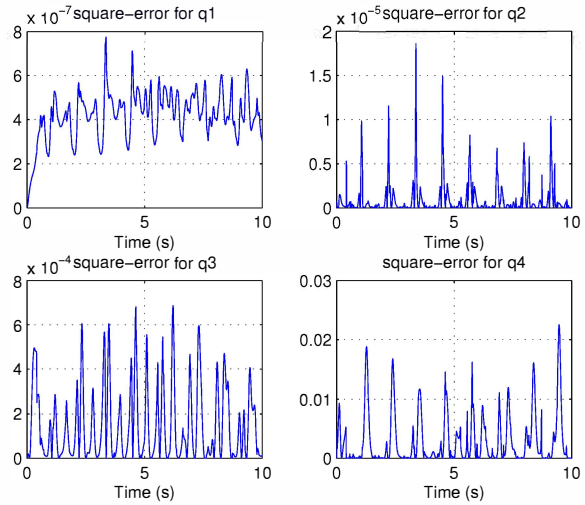

Fig. 8. Square of the tracking error (high impedance)

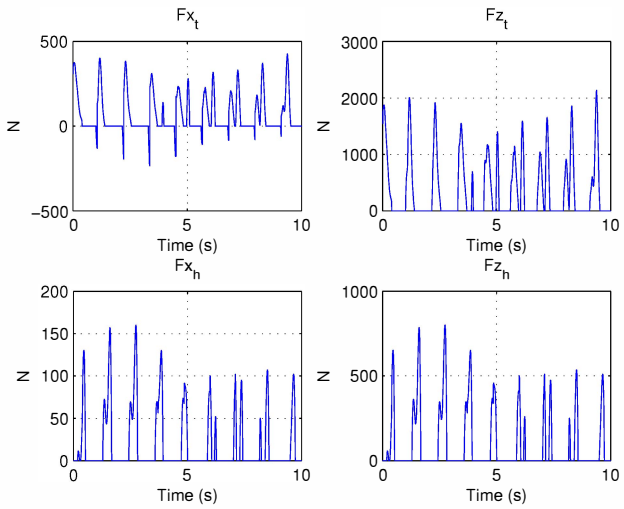

Fig. 9. Ground contact forces in heel and toe (high impedance)

tation, convergence to zero is lost and replaced by the more relaxed property of uniform ultimate boundedness. The determination of the ultimate boundedness region for the tracking error requires further study. Also, a quantification of the discrepancy between target and attained impedances with the deadzone solution remains to be studied.

In the prosthesis test robot described, impedance rather than tracking control could be used for the vertical motion of the hip, to emulate a patient's weight. However, since the hip vertical motion is unconstrained, it is difficult to select impedance parameters to avoid bouncing due to excessive deviations from the hip reference trajectory. Spring elements are frequently used in prosthetic devices to absorb forces. The proposed approach can be extended in a straightforward fashion to include joint stiffness. Also, the impedance and control parameters may be optimally scheduled, according to walking phase. Optimization objectives may include penalties on peak force, tracking errors and actuator power expenditures.

ACKNOWLEDGMENT

This work was supported by a doctoral scholarship from the Parker Hannifin Corporation and by the National Science Foundation.

REFERENCES

[1] N. Hogan, Impedance control - An approach to manipulation. Part I - Theory, *ASME Journal of Dynamic Systems, Measurement and Control*, v. 107, n1, p. 1-7, 1985

[2] N. Hogan and P. Buerger., Impedance and Interaction Control, in *Robotics and Automation Handbook*, 19,1-22, 2004

[3] N. Hogan, Force Control with A Muscle-Activated Endoskeleton. In *Advances in Robot Control*, Kawamura,S. and Svinin, M.,(Ed.), Springer Verlag, 2006

[4] J. Buchli, F. Stulp, E. Theodoro and S. Schaal, Variable impedance control, in *Robotics: Science & Systems*, 2010

[5] J. Buchli, F. Stulp, E. Theodorou and S. Schaal, An Introduction to Signal Detection and Estimation, *International Journal of Robotics Research*, v30, n7, p. 820-833, 2011.

[6] V. Duchaine and C.M. Gosselin, General Model of Human-Robot Cooperation Using a Novel Velocity Based Variable Impedance Control, in *Proc. EuroHaptics Conference and Symposium on Haptic Interfaces for Virtual Environment and Teleoperator Systems, World Haptics 2007*, p.446 - 451, 2007.

[7] R. Johansson and M.W. Spong, Optimization-based robot impedance controller design , in *Proc. 43rd IEEE Conference on Decision and Control* , v2, p.1246-1251, 2004.

[8] R. Johansson and M.W. Spong, Quadratic optimization of impedance control, in *Proc. IEEE International Conference on Robotics and Automation*, v1, p. 616-621, 1994.

[9] F. Sup, H.A. Varol, J. Mitchell, T. Withrow and M. Goldfarb, Design and control of an active electrical knee and ankle prosthesis, in *2nd IEEE RAS & EMBS International Conference on Biomedical Robotics and Biomechatronics, BioRob 2008.*, p. 523-528, 2008.

[10] E.C. Martinez-Villalpando, J. Weber, G. Elliott, H. Herr, Design of an agonist-antagonist active knee prosthesis, *2nd IEEE RAS & EMBS International Conference on Biomedical Robotics and Biomechatronics*, p. 529-534, 2008

[11] M.W. Spong, S. Hutchinson and M. Vidyasagar,Robot Modeling and Control, Wiley, 2005.

[12] J. J. E. Slotine and W. Li "On the adaptive control of robot manipulators", Int. J. of Robotics Research, vol. 6, no. 3, pp.49 -59 1987

[13] Chan, S.P., Yao, B., Gao, W.B and Cheng, M., Robust Impedance Control of Robot Manipulators, *Int. J. Robotics and Automation*, v6, n4, p. 220-227, 1991

[14] H. Richter, D. Simon, W.A. Smith and S. Samorezov, Dynamic modeling, parameter estimation and control of a leg prosthesis test robot, *Appiled Mathematical Modelling*, doi = `http://dx.doi.org/10.1016/j.apm.2014.06.006`, 2014.

[15] H. Richter and D. Simon, Robust Tracking Control of a Prosthesis Test Robot, *ASME Journal of Dyamic Systems, Measurements and Control*, v. 136, N. 3, doi:10.1115/1.4026342, 2014.

[16] F. Sup et.al., Design and Control of an Active Electrical Knee and Ankle Prosthesis, in *Proc. IEEE. RAS EMBS Int. Conf. Biomed. Robot. Biomechatron.*, p. 1949-1954, 2008

[17] F. Sup, A. Bohara and M. Goldfarb, Design and Control of a Powered Transfemoral Prosthesis, *Intl. J. Robotics Research*, v27 n2, p. 263-273, 2008.